Hindawi Publishing Corporation
Advances in Meteorology
Volume 2012, Article ID 201818, 11 pages
doi:10.1155/2012/201818

Research Article

Tracing Atlantic Water Signature in the Arctic Sea Ice Cover East of Svalbard

Vladimir V. Ivanov,[1,2,3] Vladimir A. Alexeev,[2] Irina Repina,[4] Nikolay V. Koldunov,[5] and Alexander Smirnov[1]

[1] *Arctic and Antarctic Research Institute, St. Petersburg 199397, Russia*
[2] *International Arctic Research Centre, University of Alaska, Fairbanks, AK 99775, USA*
[3] *Scottish Marine Institute, Oban PA37 1 QA, UK*
[4] *A.M. Obukhov Institute of Atmospheric Physics of RAS, Moscow 119017, Russia*
[5] *Institute of Oceanography, University of Hamburg, 20146, Hamburg, Germany*

Correspondence should be addressed to Vladimir V. Ivanov, vladimir.ivanov@sams.ac.uk

Received 7 February 2012; Revised 20 March 2012; Accepted 22 March 2012

Academic Editor: Igor N. Esau

We focus on the Arctic Ocean between Svalbard and Franz Joseph Land in order to elucidate the possible role of Atlantic water (AW) inflow in shaping ice conditions. Ice conditions substantially affect the temperature regime of the Spitsbergen archipelago, particularly in winter. We test the hypothesis that intensive vertical mixing at the upper AW boundary releases substantial heat upwards that eventually reaches the under-ice water layer, thinning the ice cover. We examine spatial and temporal variation of ice concentration against time series of wind, air temperature, and AW temperature. Analysis of 1979–2011 ice properties revealed a general tendency of decreasing ice concentration that commenced after the mid-1990s. AW temperature time series in Fram Strait feature a monotonic increase after the mid-1990s, consistent with shrinking ice cover. Ice thins due to increased sensible heat flux from AW; ice erosion from below allows wind and local currents to more effectively break ice. The winter spatial pattern of sea ice concentration is collocated with patterns of surface heat flux anomalies. Winter minimum sea ice thickness occurs in the ice pack interior above the AW path, clearly indicating AW influence on ice thickness. Our study indicates that in the AW inflow region heat flux from the ocean reduces the ice thickness.

1. Introduction

Steady reduction of the Arctic sea ice cover throughout 1990s has accelerated in the 2000s [1, 2]. As demonstrated in the recent studies, causative mechanisms for the extreme ice area/volume decay include an anomalous atmospheric circulation which forced ice out of the Canadian Basin towards Fram Strait [3, 4], the influence of warm inflow through Bering/Fram straits [5, 6], and the melting effect of warmed surface water [7]. However, long-term preconditioning occurred during three decades of steady ice thinning [8, 9]. This was largely a result of the fact that the Arctic has warmed up about twice as fast as lower latitudes due to the so-called polar amplification [10–12]. Years of reduced ice growth in winter and enhanced ice melt in summer led to the dominance of first-year ice over multiyear ice after 2004 [13].

Under conditions of enhanced seasonality, the influence of ocean heat on Arctic ice cover is expected to grow. The retreating summer ice edge increases the size of the marginal ice zones (MIZs)—the transient areas between open water and totally ice-covered ocean. For the Spitsbergen region, this process is particularly important due to the existence of an extended open water area (a quasi-steady-state polynya) bordered by an MIZ, the so-called Whalers Bay, close to the northern coast of the archipelago. In winter the presence of the large-scale open water zone substantially shapes local weather conditions, keeping air temperature well above average values for similar latitudes around the Arctic.

Large changes in the state of the ocean surface over the limited distance of MIZs build up high horizontal gradients of properties in the oceanic and atmospheric boundary layers below and above the MIZ. High gradients trigger horizontal

motions in both media, providing favourable prerequisite conditions for intensive heat, moisture, and momentum exchange across the ocean-ice-air interface. This is true for the Pacific sector (circa 120°E–120°W), where the most dramatic ice edge retreat was reported in 2007 and 2011 (http://nsidc.org/arcticseaicenews/). On the opposite side of the Arctic Ocean the ice edge deviation from the climatic mean location was substantially smaller, for example, Figure 1 in [7]. Such anisotropy indicates that despite the fact that the strongest heat input to the high Arctic is associated with the eastward moving Atlantic cyclones and warm inflow of Atlantic-origin water through the Nordic Seas, the ice cover in the Atlantic sector seems to be rather insensitive to the increased heat impact from the lower latitudes [14]. In the present study, we use observational/reanalysis data and recent findings on the properties of the Atlantic water (AW) inflow to figure out whether this is actually the case.

We focus on the region of the Arctic Ocean between Svalbard and Severnaya Zemlya archipelagos, which is further referred to as the Western Nansen Basin (WNB: 15–60°E, 81–83°N). This is an area of complex ocean-ice-atmosphere interactions resulting in isolation of the inflowing AW from direct contact with ice and atmosphere. We base our study on the hypothesis that this isolation is primarily the consequence of intensive vertical mixing at the upper AW boundary. As a result, a substantial fraction of heat is released upwards contributing to the heat budget of the under-ice water layer and impacting the ice cover. Recent findings show conservation of a strong seasonal signal in the AW temperature at the location where the warm current encounters pack ice [15]. This conservation allows extensive penetration of warm "summer" AW into the subsurface layer (above 100 m) below the pack ice. We examine spatial and temporal variation of WNB ice concentration against relevant time series of wind, air temperature, and AW temperature. The main objective of this analysis is to separate the direct dynamic influence of wind from thermodynamic effects provided by heat fluxes at the ice-air and ice-water interfaces in order to assess the relative importance of the latter.

Following the paper objective, we introduce the physical concept of AW transformation into the intermediate water mass (Section 2), describe temporal and spatial variations of WNB ice concentration from 1979–2011 (Section 3), and discuss possible links between these variations and the most probable influential factors, including wind, air temperature, and AW temperature (Section 4). Discussion of the results and major conclusions are given in Section 5.

2. Atlantic Water Transformation East of Svalbard

A schematic of the two inflow branches is shown in Figure 1. The Barents sea branch of Atlantic water (BSBW) stays at the surface while in the Barents Sea. As a result, after this water finally reaches the Arctic Ocean interior it has substantially cooled and freshened. Contrary to BSBW, the Fram Strait branch of Atlantic water (FSBW) rapidly leaves the surface,

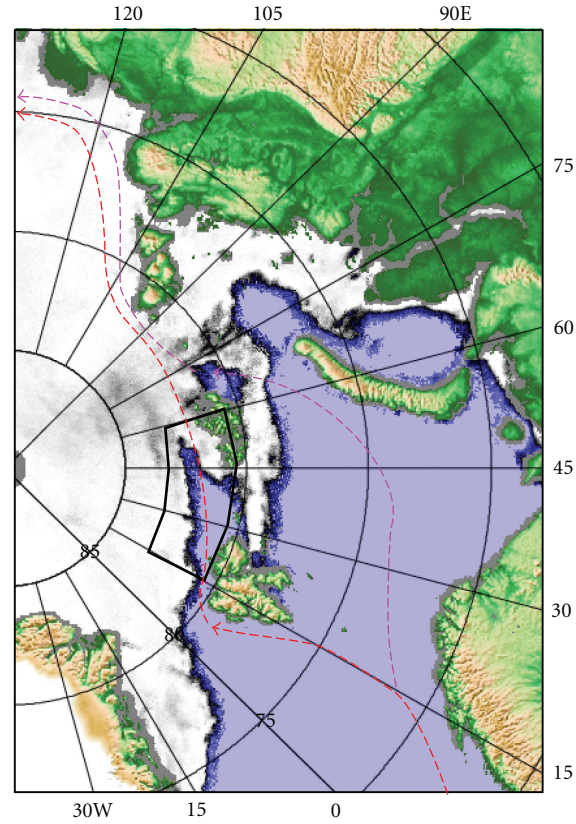

Figure 1: Schematic of two inflow branches (FSBW is shown in red and BSBW is shown in pink) of the AW against the special sensor microwave imager/Sounder (SSMIS) visual chart of ice concentration on February 4, 20112 (http://www.iup.uni-bremen.de:8084/ssmis/index.html). The Western Nansen Basin (WNB) area is marked by a black trapezium.

transforming into Arctic intermediate water (AIW). Due to this separation from the surface, AIW retains a large amount of its initial heat and salt, which are further transported around the deep ocean interior.

According to the Arctic Ocean climatology, north of Svalbard FSBW is capped by a cold and relatively fresh mixed water layer all year round [16]. The origin of this mixed layer is still under discussion. The traditional hypothesis states that this layer contains Arctic surface water which moves generally towards Fram Strait, opposing the FSBW inflow. Since this water is lighter than FSBW, it overlays the latter causing FSBW to sink beneath the surface mixed layer [17]. Westward flow in the surface mixed layer is consistent with the large-scale ice motion observed in the Arctic Ocean, for example Figure 1(e) in [18]. An alternative hypothesis suggests that the surface mixed layer originates directly in the upper part of inflowing AW, which cools down via heat loss to the atmosphere and freshens due to mixing with melted ice water [19]. This newly formed surface layer follows the warm bulk of AIW moving eastward along the continental slope, except for a very thin under-ice layer, which is deflected westwards by the drifting ice. Basically, both hypotheses agree that there must be some depth inside

the water column at which the current turns around. The difference between these hypotheses is the depth at which this change of direction occurs. Observational data collected using traditional oceanographic methods, like occasional conductivity/temperature/depth (CTD) profiling at a limited number of transects, does not provide reliable justification for either of these hypotheses. For example, the typical inclination of isotherms between Svalbard and Franz Joseph Land (Figure 2) may be caused either by submerging of the AW water as it travels from west to east, or by cooling of the upper part of AW en route.

Recent measurements made at the autonomous moored station within the framework of the Nansen and Amundsen Basins Observational System (NABOS) project (http://www.iarc.uaf.edu/nabos.php) revealed strong seasonal variability in the inflowing FSBW (Table 1), which is conserved in the AIW far to the east of Fram Strait [20]. We suggest that this new knowledge provides some clue to understanding the FSBW transformation process. Applying the data from Table 1, we estimate that to increase the temperature of the $H = 217$ m thick layer over a unit square by $\Delta\overline{T} = 4.76$ K (the difference between the May and November vertically averaged temperature, under the assumption that the ocean surface is permanently at the freezing point), 4.2×10^9 J of heat is required (using the specific heat of sea water at constant pressure, $c_p = 4 \times 10^3$ J/kg/K and water density $\rho = 1.028 \times 10^3$ kg/m^3). Where does this heat come from? A crucial difference between the Arctic Ocean interior and the waters to the south is that summer warming due to the flux at the sea surface is tiny in the Arctic and is limited to a thin surface layer. A substantial part of the absorbed heat is spent on ice melting, thus it contributes little to the net water temperature increase. Therefore, the observed seasonal increase of heat content could only be caused by advection of warmer water, and not by the local ocean-air energy exchange. In contrast, seasonal cooling might be attributed to high negative local heat loss, which overcomes the positive advective influx.

The heat balance equation in the finite differences form may be written as follows:

$$c_p \rho H \frac{\Delta\overline{T}}{\Delta t} = Q - A, \tag{1}$$

where Δt is the time interval, Q is the heat flux due to all nonadvective processes, and A is the heat flux caused by advection. Presuming that A is always negative, that is, the water coming from the west is warmer than the water at the position of the mooring, the change of sign on the left side of (1) is determined by Q. Positive $\Delta\overline{T}/\Delta t$ means that $Q - A > 0$. This is what happens in the warming season. During the cooling season, $Q - A < 0$. As shown in [15], the most probable reason for high negative Q in winter is thermal convection, which in the area of Whalers Bay (north of Svalbard) is able to reach deep into the water column [21].

Using the data from Table 1, and considering the water at the ocean surface to be permanently at the freezing point temperature, we can estimate heat loss from the upper 217 m, under the assumption of small seasonal variation of advection [15]. Substituting vertically averaged temperature change between April-May and November in (1) and neglecting Q yields A equal to -235 W/m^2. Using this number for the cooling phase and taking into account the difference between the duration of warming and cooling seasons, we obtain an average heat loss of 560 W/m^2. This is a huge heat loss, having the same order of magnitude as is typically estimated for Arctic winter polynyas [22]. This number also matches well with the heat flux calculations done for the MIZ in the Barents Sea in winter [23]. Aagaard et al. [21] estimated winter heat loss in Whalers Bay from the 100–200 m layer to be 230 W/m^2. Applying the same equation (1) for the 113–217 m layer yields a similar result, 220 W/m^2. In the light of these numbers, the estimate done in [24], suggesting an increased surface heat loss of about 300 W/m^2 during pulses of anomalously warm AW inflow through Fram Strait, is also quite reasonable.

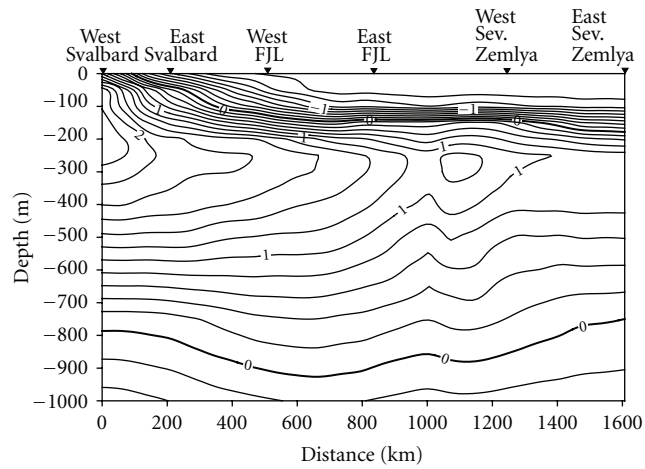

Figure 2: Temperature, °C section along the FSBW inflow in summer season (EWG, 1998) (FJL: Franz Joseph Land).

Progressive vector diagrams close to the core of the boundary current at 30°E calculated on the basis of 1-year-long continuous current meter measurements with 1-hour resolution show that the entire 70–217 m water layer is moving generally eastward with an average speed of 12–17 cm/s [15]. This indicates that the opposite motion (towards Fram Strait) may occur only in the subsurface layer above 70 m depth. The water at this level is apparently AW all year round despite the fact that its temperature may drop down to the freezing point. The AW "signature" is identified not by characteristic temperature and salinity values, but by the constant shape of the temperature-salinity (T-S) relationship [15]. Taking into account the steadiness of the flow direction and speed, we can argue that the actual cutoff depth of the reverse current is shallower than 70 m. Another argument in favor of this notion follows from the vertical distribution of temperature and salinity at cross-slope sections near the mooring position, see Figure 2 in [15]. In September 2006, the warm water core (over 5°C) resided at 50 m, while positive temperature water spread up to the ocean surface. A sharp salinity gradient at the 25–30 m depth

Table 1: Amplitude and phase of seasonal cycle in water temperature at 80°30′N and 31°E [15].

Depth (m)	Maximum, daily data		Minimum, daily data	
	Date	(T) °C	Date	(T) °C
70 ± 5	Nov 16 ± 10	5.12 ± 0.12	Apr 13	−1.77 ± 0.05
113 ± 5	Nov 16 ± 8	4.81 ± 0.17	Apr 23 ± 3	−0.40 ± 0.33
217 ± 5	Nov 24 ± 17	4.27 ± 0.29	May 13 ± 2	2.02 ± 0.06

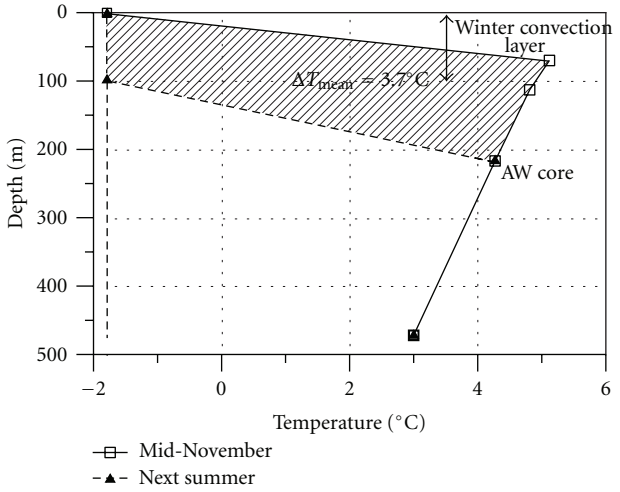

Figure 3: Sketch of the upper FSBW transformation during the winter season.

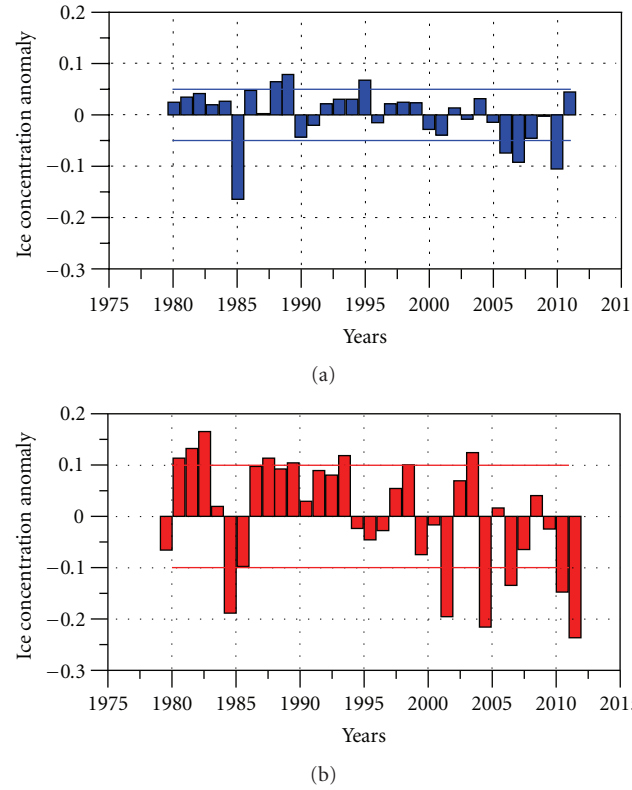

Figure 4: Time series of ice concentration (in parts of the unit) in the WNB (winter: blue; summer: red).

marks the location of the AW upper boundary in the vertical plane. The shape of the T-S relationship inside the 30–70 m layer also matches very well the typical AW T-S relationship, indicating that the water in this layer contains a considerable AW fraction.

The strong seasonal variation of heat content in the upper part of the water column at the mooring position in conjunction with the eastward direction of flow implies that a substantial amount of heat is advected by the boundary current. A persistent current moves warm water further to the east, bringing the upper part of this warm layer into close contact with pack ice drifting in the opposite direction. Taking into account that further to the east (in the Laptev Sea) the upper boundary of AW deepens to 150–200 m, we can anticipate that the heat stored above this depth is released en route, warming the under-ice layer. Applying simple theoretical considerations to the mid-November temperature profile from Table 1 enables us to estimate the order of magnitude of heat loss from the upper part of the water column. The evolution of temperature from mid-November to the following summer is sketched in Figure 3. Presuming that winter convection depth in the WNB is about 100 m [25], we calculate a mean temperature decrease above the AW core of 3.7°C. Applying this decrease of temperature to six winter-spring months yields a total heat loss of about 200 W/m^2. If only 7% of this heat goes upward [6], we calculate the value of heat flux from the ocean to the ice to be 7 times larger than the conventional mean value [26]. This estimation points out that a considerable portion of seasonal heat input into the upper part of the WNB water column might be spent on ice melt and released to the atmosphere.

3. Structure and Variability of WNB Ice Conditions from 1979–2011

Data on ice concentration were taken from the Nimbus-7 Scanning Multichannel Microwave Radiometer (SMMR), and the Defense Meteorological Satellite Program (DMSP) Special Sensor Microwave/Imager (SSM/I), and Passive Microwave Data dataset [27, http://nsidc.org/data/nsidc-0051.html]. A brief description of these data is given in the Appendix. Time series of mean spatial winter and summer ice concentration (MSIC) in parts of the unit in the WNB are presented in Figure 4. Winter season was defined from November 1 to May 31 and summer season

from June 1 to October 31. In winter, average MSIC is 0.88 ± 0.05, while in summer, it is 0.72 ± 0.10. Statistical properties are not uniform across time. Two distinct periods can be seen, with the border between them around 1995–1999. During the 1st time interval (1979–1995), positive MSIC anomalies prevail. There are 13 positive anomalies versus 3 negative in winter season and 12 positive versus 4 negative in summer. Values of anomalies lie within, or slightly exceed simple standard deviation (SSD) bounds. The only exception is the year 1985, which is characterized by large and coherent summer-winter negative anomalies. Anomalies exceed the SSD about twice in summer and more than 3 times in winter. During the 2nd time interval (1999–2011), the general pattern of anomalies is the opposite. In winter there are 8 negative anomalies versus 3 positive, while in summer there are 9 negative anomalies versus 4 positive. The negative anomalies often substantially exceed SSD, especially in summer. Although the time series are too short for performing robust correlation analysis, formal calculation shows that the correlation coefficient between the preceding summer and the next winter anomaly drops from 0.5 (in 1979–1995) to 0.1 (in 1999–2011). This suggests that the processes which control ice concentration during time intervals with high and low ice concentrations are not the same.

The difference between the average ice concentrations during two selected periods are plotted in Figure 5. In both seasons, ice concentration decreased during the 2nd time interval over the entire WNB area. In summer the maximum ice concentration decrease (−0.3) occurs within the WNB. Further to the north, the difference between the two time intervals is close to zero. The latter is explained by the fact that the region to the north of 83°N in the Atlantic sector of the Arctic Ocean is the "pack ice collector" for the new ice forming in Siberian shelf seas and being driven towards Fram Strait in the Transpolar Drift system [17]. In winter season the largest differences extend along two branches of AW (compare with Figure 1). During the 2nd time interval low-concentration "tongues" associated with two branches of AW merge, forming the large area with decreased ice concentration in the northern part of the Barents Sea and over the continental margin of the Nansen Basin (this plot is not shown).

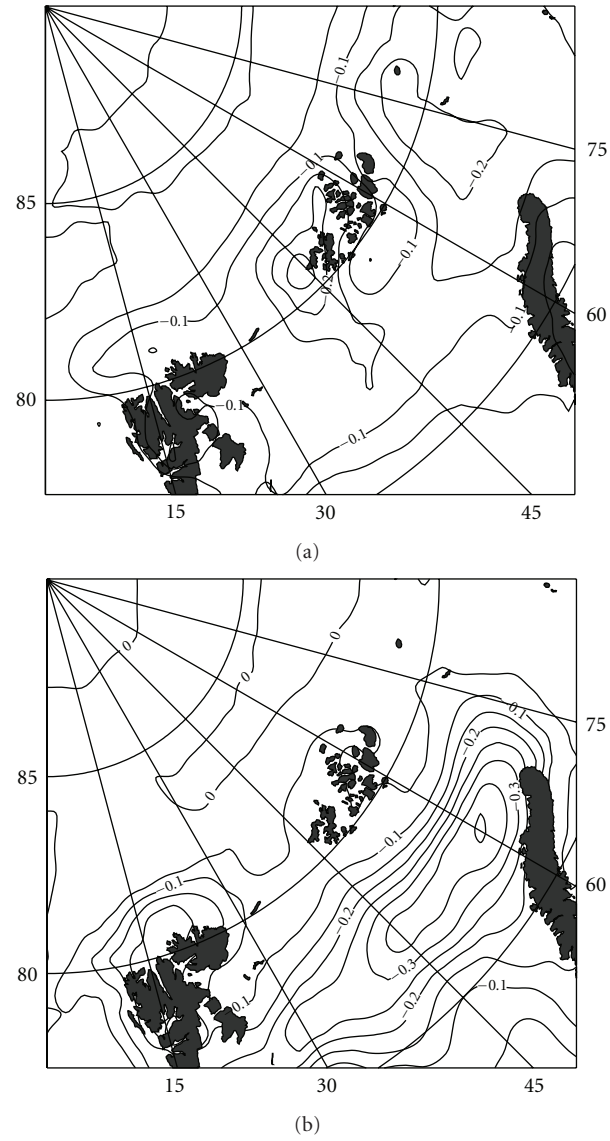

Figure 5: Difference between the average ice concentrations in the WNB in 1999–2011 versus in 1979–1995 in summer (a) and in winter (b).

In line with our basic hypothesis, which implies a substantial contribution of oceanic sensible heat in shaping the ice cover in the WNB (see Figure 1), we considered the unique ice thickness measurements made within the framework of the Ice, Cloud, and land Elevation Satellite (ICESat) campaigns [[28] http://rkwok.jpl.nasa.gov/icesat/download.html]. Two sequential maps showing ice thickness in October-November, 2007 (ON2007) and February-March, 2008 (FM2008) are presented in Figure 6. Our choice of 2007-2008 is dictated by the record summer minimum ice extent in the Arctic Ocean in 2007. Despite the record retreat of the ice edge in the Pacific sector, summer ice extent in the WNB was close to normal, which is reasonably explained by dynamics [29]. The FSBW pathway along the continental slope between Svalbard and Franz Joseph Land is within the seasonal summer MIZ; this does not provide any arguments for or against the hypothesis that AW heat impacts ice properties. A very different picture appears during the next winter survey (Figure 6(b)). The ice edge is shifted far to the south of the WNB. However, the local minimum ice thickness, surrounded by thicker ice, stretches from Svalbard to Severnaya Zemlya Archipelagos, visibly marking the FSBW inflow pathway.

Putting together the revealed features of mean seasonal distribution and interannual variability of ice concentration in the WNB and ice thickness data from 2007-2008, we suggest the following. The spatial patterns of ice distribution in winter and in summer are not the same. In winter, zones of decreased ice concentration extend along the branches of AW inflow, while in summer ice concentration decreases uniformly northward. Summer and winter MSIC

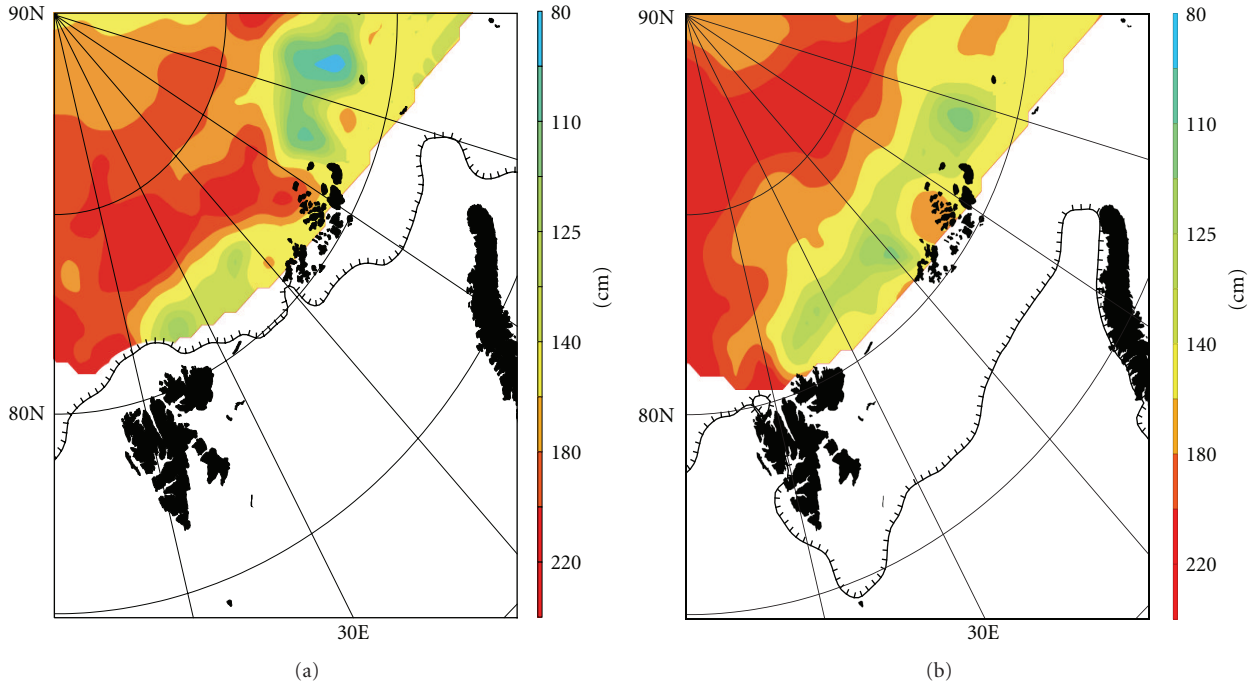

Figure 6: October-November, 2007 ice thickness (a); February-March, 2008 ice thickness (b). Black solid lines show the location of the ice edge, defined by 15% ice concentration.

time series are divided into two specific intervals: 1979–1995, with generally higher ice concentration and 1999–2011, with generally lower ice concentration. During the 1st time interval, the winter MSIC inherits features of the preceding season (summer-winter correlation coefficient is equal to 0.5). During the 2nd time interval, there is no link between summer and winter ice concentrations. Available ice thickness measurements support the notion that a substantial amount of heat reaches the under-ice surface and melts ice from below, rendering it thinner and more fragile. This process is especially noticeable in the winter season, when most of the Arctic Ocean is ice covered. In the next section, we test this observation-based hypothesis against available oceanographic and meteorological data and atmospheric reanalysis products in a search for the causative mechanisms that shape the sea ice cover in the WNB.

4. Causative Mechanisms

To elucidate possible mechanisms responsible for the observed features of the WNB ice conditions, we consider the following time series: (i) FSBW temperature at the WNB entry point; (ii) meridional wind component over the WNB; (iii) air temperature and surface-air temperature difference; (iv) sensible heat flux at the ocean surface. For this task, we used reanalysis products (http://www.ecmwf.int/research/era/do/get/era-interim). The features of this data set are briefly described in the Appendix.

FSBW interannual variability near the entry point. Annual time series of AW temperature were generated inside the cell bounded by 78–80°N and 5–10°E. This is the mean climatic position of the West Spitsbergen Current main stream, see Figure 3 in [24]. The data from the Arctic and Antarctic Research Institute (AARI) collection were used [30]. We consider two water layers: 100–200 m and 200–300 m (Figure 7). This choice is explained by the features of AW transformation in the AIW discussed in Section 2. Provided that the concept of AW intensive mixing in the upper part is correct the layer shallower than ~200 m initially contains the heat, which is totally released upwards and laterally during the FSBW transit from Fram Strait to the Laptev Sea. The layer below ~200 m retains a large portion of its initial heat content up to where the AIW terminates its full circuit around the Arctic Ocean interior. Within the considered time interval (1979–2011) the temperature in both AW layers coherently increased. However, this increase was not monotonic, but rather cyclic with an 8–10-year period. The background positive trend is 1.5° per 32 years in the upper layer and 1.25° per 32 years in the lower layer. It is worth mentioning that after the most recent temperature increase, which culminated in 2007, the temperature did not drop back to the initial point as happened earlier, but remained about 1°C higher in both layers, leading to the conclusion that AW in the Arctic Ocean is shifting to a new warmer state [31, 32]. Hence, there is no doubt that the heat input to the Arctic Ocean interior has substantially increased since the end of the 1990s. The question is has this increased heat input provided the major forcing of the documented change in ice properties in the WNB? To answer this question let us examine the other potentially significant mechanisms.

Wind stress is usually considered to be the primary forcing which creates open water zones in the consolidated ice cover in winter [33]. Well-known quasi-steady-state

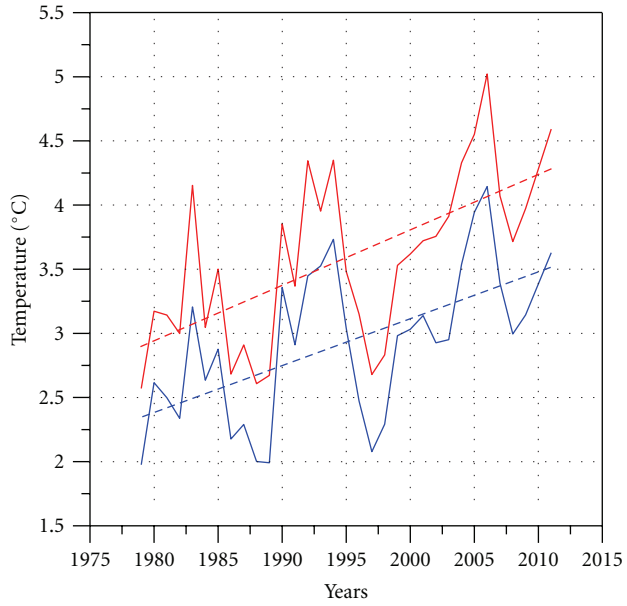

Figure 7: Water temperature in the core of the West Spitsbergen current at 79°N; red: 100–200 m layer; blue: 200–300 m layer.

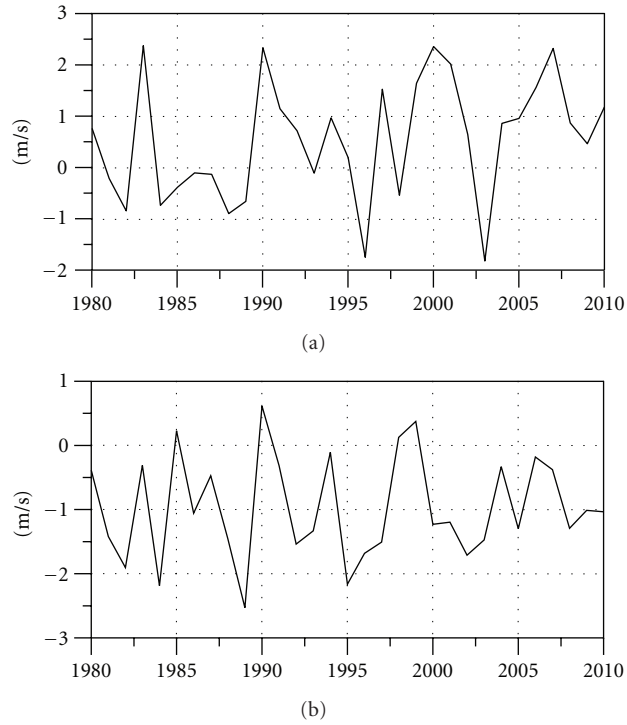

Figure 8: Meridional wind component in winter around Franz Joseph Land (a) and north of Svalbard (b).

polynyas along the Eurasian and American coastline are formed by katabatic wind and local currents which break up the fast ice and drive ice floes offshore [34]. In the conventional terminology such a polynya is known as a latent heat polynya (LHP) [35]. Another type of polynya, the sensible heat polynya (SHP), is thermodynamically driven and typically occurs when warm water upwelling keeps the surface water temperature above the freezing point. Favorable wind may also assist in maintaining an open SHP, but the major role is played by oceanic heat. To determine whether variation of the WNB open water area in winter is caused by wind stress, we plotted the time series of the meridional surface wind component in two localized regions where an increased area of open water was observed during the 2nd time interval (see Figure 8). No visible trends in the meridional wind component can be inferred from this plot or from the time series of wind speed (not shown), thus removing wind from the list of likely causative mechanisms.

Air temperature variation is another obvious candidate to be linked with the observed changes in the ice cover. In Figure 9, one can see that air temperature changed around the mid-1990s, at which time air temperature started to increase almost monotonically, which is in line with the ice concentration change. At about the same time the air-surface temperature difference decreased and then stayed at almost the same level up until present with a very weak upward tendency (Figure 10).

Wind speed and air-surface temperature difference determine sensible *heat flux* at the ocean ice/air interface [36]. In the absence of short-wave radiation (in winter season), sensible heat flux is the major contributor to the surface-air energy balance. The shape of the sensible heat flux curve in winter season (Figure 11) is very similar to the air-sea temperature difference curve, with a tipping point around 1995. However, it is important to note that the sensible heat flux shows more of a tendency to increase than does the air-surface temperature difference after 1995.

5. Discussion and Conclusions

Our analysis of WNB ice properties from 1979–2011 allowed us to detect a general tendency towards decreasing ice concentration that commenced after the mid-1990s. Combining the ice concentration data and the available ice thickness data allowed us to demonstrate that the location of local zones with thinner ice and lower ice concentration essentially mirror the pathway of the FSBW in the WNB. Time series of FSBW temperature in Fram Strait feature a monotonic increase after the mid-1990s, consistent with shrinking ice cover. This coincidence provides solid ground for the hypothesis that a substantial amount of the AW heat in the WNB is able to reach the under-ice layer and contribute to the ice melting from below. On the other hand, there is evidence in reanalysis products that WNB air temperature has exhibited trends consistent with those of ice concentration and FSBW temperature. Therefore, the question to pose is as follows. Are one or more of these correlated processes drive the observed changes, or is the driver of something else entirely? To answer this question let us briefly outline the physical background of ocean-ice-air interaction. In the ice-covered seas a key factor controlling the rate of energy exchange is the spatial irregularity of the ice cover. Irregularity primarily depends on the ice concentration and thickness [37]. Under similar

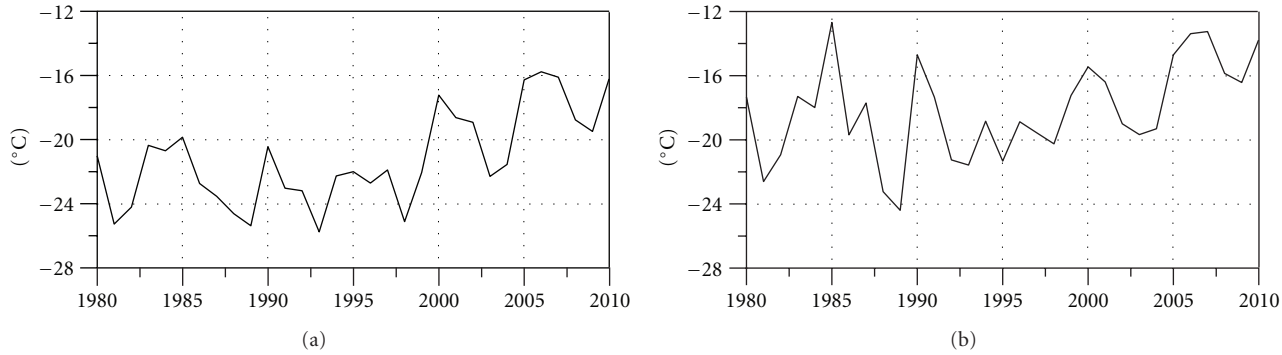

Figure 9: Air temperature at the surface in winter around Franz Joseph Land (a) and north of Svalbard (b).

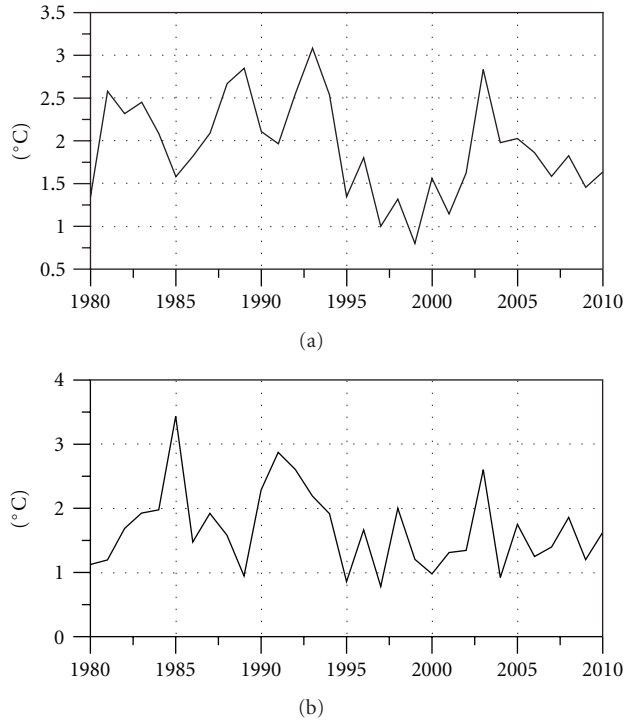

Figure 10: Surface-air temperature difference in winter around Franz Joseph Land (a) and north of Svalbard (b).

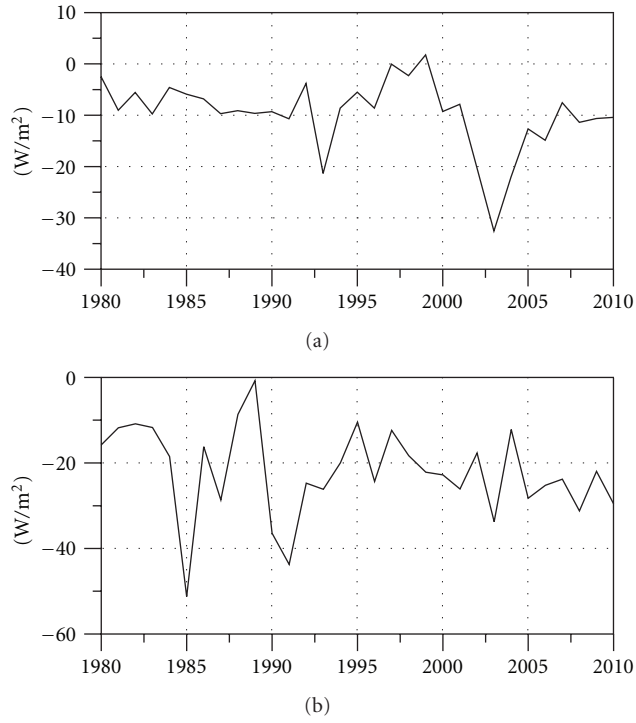

Figure 11: Sensible heat flux at the ocean ice/air interface in winter around Franz Joseph Land (a) and north of Svalbard (b).

meteorological conditions, heat exchange through the ice-free surface is two orders of magnitude greater than that through the surrounding pack ice [35]. Turning back to Figures 6, 7, and 8, we draw attention to the following facts. Air temperature permanently increased after the mid-1990s, as did negative sensible heat flux. Therefore, the amount of heat released from the ocean to the atmosphere increased. At the same time, the air-surface temperature difference did not show any significant trend. European reanalysis (ERA-Interim) surface heat fluxes from partially ice-covered ocean are obtained by averaging fluxes over open water and ice proportionally according to the concentration in a given model cell. Therefore, we argue that an increase of sensible heat flux from the ocean after the mid-1990s is a result of lower sea ice concentration in the area (perhaps due to an increased number of small-scale leads [38]). Lower sea ice concentration is the consequence of ice thinning under the influence of an increased sensible heat flux from AW because ice erosion from below enables more effective breaking of the thinner ice by wind (which has not visibly changed) and by local currents. Lower sea ice concentrations are collocated with areas of anomalies in the surface heat fluxes (Figure 12). The fact that the minimum sea ice thickness lies in the interior of the ice pack right above the FSBW path (see Figure 6(b)) is a clear indication of the influence of heat flux from the FSBW on ice thickness. The physical processes that deliver warm water from the deep to the under-ice layer are yet to be studied in detail. We assume that in the study area the most likely candidate is winter convective mixing. In the WNB, in the absence of a cold halocline, convective

mixing reaches the depth of ~100 m [25], entraining the upper part of AW, which is at its seasonal peak in late fall—early winter [15]. Additional forcing could be provided by upwelling events at the continental slope of Franz Joseph Land [39] and/or by Ekman pumping [14].

The possibility of AW heat impact on the Arctic Ocean ice cover has been debated since Fritjof Nansen's 1890s discovery of a warm water layer under the pack ice. The hypothesis that AW affects ice properties always had its supporters and opponents. However, the absence of robust observational data in specific locations and specific seasons prevented this dispute from growing beyond theoretical speculations and indirect estimations to justified statements, based on observations. In the present study we demonstrate that in the WNB region AW directly affects the ice thickness, providing an efficient thermodynamic mechanism by which ice volume is decreased. The significance of this influence in the pan-Arctic sea ice and fresh water budgets should be the subject of future studies.

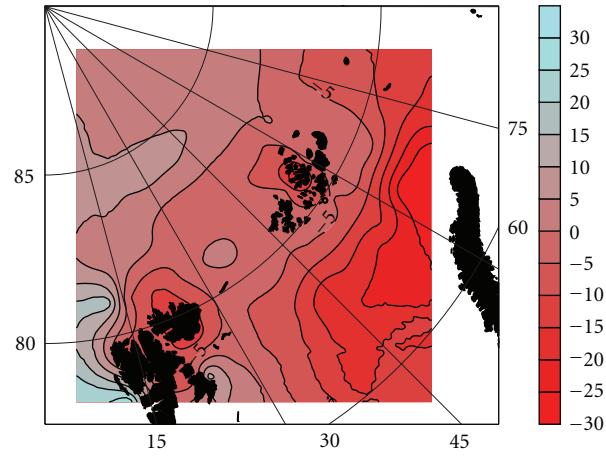

Figure 12: Averaged 1980–2010 winter distribution of sensible heat flux at the surface, W/m^2 (a); difference in heat flux between 1999–2010 and 1980–1995 (b).

Appendix

Data Sources and Uncertainties

For this study we used publicly available data sets. Originators of these data sets provide detailed description of metadata, including methods of measurements, accuracy, and so forth. Here, we briefly describe the sources of data and discuss possible uncertainties in the presented results.

CTD and mooring-based data on WNB temperature and salinity were taken from the NABOS data archive (http://nabos.iarc.uaf.edu/). These data had passed thorough quality control and have been used in multiple published studies, see [40]. The *AW temperature* in Fram Strait has been monitored for an extended period of time by the international scientific community, mainly by Russian, Norwegian, and German researchers [14, 24, 41]. The AW time series used in this study were generated from the oceanographic data base, collected, and routinely complemented by new data at the Arctic and Antarctic Research Institute (AARI). *Ice concentration* data were taken from the Nimbus-7 Scanning Multichannel Microwave Radiometer (SMMR) and the Defense Meteorological Satellite Program (DMSP) Special Sensor Microwave/Imager (SSM/I) Passive Microwave Data dataset [27, http://nsidc.org/data/nsidc-0051.html]. The spatial resolution of the regular grid is 25 km. For the year 2011, preliminary data from this dataset were used [42]. We calculated 10 day averages from the daily data and used the resulting products for the analysis. *Ice thickness* data were taken from the ICESat data collection [28] 2008; (http://rkwok.jpl.nasa.gov/icesat/download.html). *Meteorological* data and derived parameters (heat fluxes) were taken from the ERA-Interim reanalysis (http://www.ecmwf.int/research/era/do/get/era-interim). ERA-Interim is the latest ECMWF global atmospheric reanalysis covering the period from 1979 to present. It uses 4D variational data assimilation of a wide variety of observations from surface based to aerological and satellite measurements. Available fields include all major meteorological variables plus important surface diagnostics including surface fluxes. We use the 1.5 × 1.5 degree resolution version of ERA Interim available from the ECMWF web site: http://www.ecmwf.int/.

Uncertainties are an inseparable component of any observation-based investigation, and our study is not free of them. We recognize two types of uncertainties: (i) uncertainties associated with the limitation of the data used and (ii) uncertainties caused by simplifications introduced during the analysis. Uncertainties in hydrographic data are usually caused by changing the location of sequential CTD casts and low horizontal resolution. Since the NABOS CTD data that we used were collected at the recurrent cross-slope section with ~5 km distance between stations over the steepest part of the slope, we do not expect a noticeable error in estimation of AW properties. Mooring-based data were collected close to the core of the AW flow, as was shown in [15], which also guarantees small errors of estimation based on these data. Uncertainties in ice concentration data were discussed in [43]. They conclude that according to data documentation in general, the accuracy of total sea ice concentrations is within ±5% of the actual sea ice concentration in winter, and ±15% in the Arctic during summer when melt ponds are present on the sea ice. Although these numbers are close to the MSIC variations presented in Figure 4, we would like to stress our use of ice concentration data averaged over time and space, which reduces the error proportional to the square root of the number of individual measurement points. Ice concentration data (as well as ice thickness data) have rather crude spatial resolution (25 km) and do not resolve small openings in the ice cover (cracks and flaw leads). However, for the purpose of the presented analysis these data fit reasonably well, since we discuss relatively large (~hundreds of kilometers) features. Uncertainty in the diagnostic fields provided by ERA-Interim, which are not constrained by any sort of data assimilation procedures, is always a big problem for any

reanalysis products. For example, in [44] it is discussed that the overall performance of ERA-Interim products including fluxes over ocean. They found that the quality of many diagnosed variables (e.g., precipitation and surface fluxes) greatly improved in ERA-Interim in comparison with other products of this kind.

Uncertainties in the presented analysis may be associated with our failure to take ice drift into account. Drift provides key forcing of ice redistribution. We checked the pattern of ice thickness anomalies against the mean ice drift in February-March 2008 [18]. Within this time interval, mean ice drift in the WNB and around it was generally directed southward with speed not exceeding 5 km/day. Therefore, we conclude that the error of failing to take ice drift into account may not noticeably affect our results. Another possible source of error in ice thickness estimation is snow on ice, which is difficult to assess. Since large-scale snow anomalies are collocated with downwelling long wave (DLW) radiation, we estimated total accumulated snowfall from the ERA-Interim dataset by assuming snow density of 0.25, and that snowpack starts developing in September. No correlation between snowfall anomalies and ice thickness anomalies in 2008 was found. ERA-Interim uses satellite observed sea ice concentrations to calculate surface fluxes over the Arctic Ocean. Small-scale features like cracks and polynyas may not be well resolved. However, if sea ice concentration is less than 100% in a grid cell, open water and sea ice are calculated separately. The total heat flux over the grid cell is then calculated according to the proportion of open water and sea ice in that grid cell. Absolute values of air-surface temperature difference decreased according to our analysis. Since the wind change is relatively small, this could only lead to a decrease in the sensible heat flux if the surface properties stayed the same (e.g., ocean remained ice covered). Therefore, sensible heat flux can increase only at the expense of more open water in the area, because heat fluxes from open water are far greater than fluxes over ice-covered ocean. Note that we use the ERA-Interim sign convention: negative surface heat flux means the surface is heating the atmosphere.

We acknowledge that the presented analysis may be not perfect because the available data sets have limitations. However, we believe that the uncertainties of data and analytical method do not call into question the conclusions of this paper.

Acknowledgments

This study was supported by the following research grants/programs: EU FP7 "Arctic Climate Change Economy and Society" (ACCESS) project, NERSC-IAP 196174/S30: "The atmospheric boundary layer structure and surface-atmosphere exchange in the Svalbard area;" RFBR 11-05-12019-ofi-m-2011: "Modern polar climate change estimation on the base satellite microwave database GLOBAL-RT;" RFBR 11-05-01143: "Investigation of tide action on generation and dynamics of internal waves and their manifestation on the sea surface in Russian Arctic seas;" ONR-Global grant 62909-12-1-7013: "Decision Making Support System for Arctic Exploration, Monitoring and Governance;" European Commission 7th framework program through the MONARCH-A Collaborative Project, FP7-Space-2009-1 Contract no. 242446, NSF Grant ARC 0909525 and Japan Agency for Marine-Earth Science and Technology. ERA-Interim data used for the analysis were downloaded from the website of the European Centre for Medium Range Weather Forecasts (http://www.ecmwf.int/). The authors thank Anton Beljaars of ECMWF for providing very useful information on ERA-Interim data assimilation procedures.

References

[1] J. C. Comiso, C. L. Parkinson, R. Gersten, and L. Stock, "Accelerated decline in the Arctic sea ice cover," *Geophysical Research Letters*, vol. 35, no. 1, Article ID L01703, 2008.

[2] M. Wang and J. E. Overland, "A sea ice free summer Arctic within 30 years?" *Geophysical Research Letters*, vol. 36, no. 7, Article ID L07502, 2009.

[3] B. Y. Wu, J. Wang, and J. E. Walsh, "Dipole anomaly in the winter Arctic atmosphere and its association with sea ice motion," *Journal of Climate*, vol. 19, no. 1, pp. 210–225, 2006.

[4] V. A. Alexeev, I. N. Esau, I. V. Polyakov, S. J. Byam, and S. Sorokina, "Vertical structure of recent Arctic warming from observed data and reanalysis products," *Climatic Change*, vol. 111, no. 2, pp. 215–239, 2011.

[5] K. Shimada, T. Kamoshida, M. Itoh et al., "Pacific Ocean inflow: influence on catastrophic reduction of sea ice cover in the Arctic Ocean," *Geophysical Research Letters*, vol. 33, no. 8, Article ID L08605, 2006.

[6] I. V. Polyakov, L. A. Timokhov, V. A. Alexeev et al., "Arctic ocean warming contributes to reduced polar ice cap," *Journal of Physical Oceanography*, vol. 40, no. 12, pp. 2743–2756, 2010.

[7] D. K. Perovich, J. A. Richter-Menge, K. F. Jones, and B. Light, "Sunlight, water, and ice: extreme Arctic sea ice melt during the summer of 2007," *Geophysical Research Letters*, vol. 35, Article ID L11501, 4 pages, 2008.

[8] D. A. Rothrock, Y. Yu, and G. A. Maykut, "Thinning of the Arctic Sea-Ice cover," *Geophysical Research Letters*, vol. 26, no. 23, pp. 3469–3472, 1999.

[9] J. Rodrigues, "The rapid decline of the sea ice in the Russian Arctic," *Cold Regions Science and Technology*, vol. 54, no. 2, pp. 124–142, 2008.

[10] V. A. Alexeev, P. L. Langen, and J. R. Bates, "Polar amplification of surface warming on an aquaplanet in "ghost forcing" experiments without sea ice feedbacks," *Climate Dynamics*, vol. 24, no. 7-8, pp. 655–666, 2005.

[11] P. L. Langen and V. A. Alexeev, "Polar amplification as a preferred response in an idealized aquaplanet GCM," *Climate Dynamics*, vol. 29, no. 2-3, pp. 305–317, 2007.

[12] R. V. Bekryaev, I. V. Polyakov, and V. A. Alexeev, "Role of polar amplification in long-term surface air temperature variations and modern arctic warming," *Journal of Climate*, vol. 23, no. 14, pp. 3888–3906, 2010.

[13] R. Kwok, C. F. Cunningham, M. Wesnahan, I. Rigor, H. J. Zwally, and D. Yi, "Thinning and volume loss of the Arctic Ocean ice cover: 2003–2008," *Journal of Geophysical Research*, vol. 114, Article ID C07005, 16 pages, 2009.

[14] S. Lind and R. B. Ingvaldsen, "Variability and impacts of Atlantic water entering the Barents sea from the north," *Deep Sea Research I*, vol. 62, pp. 70–88, 2011.

[15] V. V. Ivanov, I. V. Polyakov, I. A. Dmitrenko et al., "Seasonal variability in Atlantic Water off Spitsbergen," *Deep-Sea Research I*, vol. 56, no. 1, pp. 1–14, 2009.

[16] Environmental Working Group (EWG), *1998, Joint U.S.-Russian Atlas of the Arctic Ocean (CD-ROM)*, National Snow and Ice Data Center, Boulder, Colo, USA, 1997.

[17] Y. G. Nikiforov and A. O. Shpaikher, *Features of the Formation of Hydrological Regime Large-Scale Variations in the Arctic Ocean*, Gydrometeoizdat, Leningrad, Russia, 1980.

[18] R. Kwok and J. Morrison, "Dynamic topography of the ice-covered Arctic ocean from ICESat," *Geophysical Research Letters*, vol. 38, Article ID L02501, 6 pages, 2011.

[19] B. Rudels, E. P. Jones, L. G. Anderson, and G. Kattner, "On the intermediate depth waters in the Arctic ocean," in *The Polar Oceans and Their Role in Shaping the Global Environment*, O. M. Johannessen, R. D. Muench, and J. E. Overland, Eds., pp. 33–46, AGU Geophysical Monograph 85, Washington, DC, USA, 1994.

[20] I. A. Dmitrenko, S. A. Kirillov, V. V. Ivanov et al., "Seasonal modification of the Arctic Ocean intermediate water layer off the eastern Laptev Sea continental shelf break," *Journal of Geophysical Research C*, vol. 114, no. 6, Article ID C06010, 2009.

[21] K. Aagaard, A. Foldvik, and S. R. Hillman, "The west spitsbergen current: disposition and water mass transformation," *Journal of Geophysical Research*, vol. 92, no. C4, pp. 3778–3784, 1987.

[22] M. A. Maqueda, A. J. Willmott, and N. R. T. Biggs, "Polynya dynamics: a review of observations and modeling," *Reviews of Geophysics*, vol. 42, no. 1, Article ID RG1004, 37 pages, 2004.

[23] S. Hakkinen and D. J. Cavalieri, "A study of oceanic surface heat fluxes in the Greenland, Norwegian, and Barents Seas," *Journal of Geophysical Research*, vol. 94, no. 5, pp. 6145–6157, 1989.

[24] U. Schauer, E. Fahrbach, S. Osterhus, and G. Rohardt, "Arctic warming through the fram strait: oceanic heat transport from 3 years of measurements," *Journal of Geophysical Research C*, vol. 109, no. 6, Article ID C06026, 14 pages, 2004.

[25] B. Rudels, E. P. Jones, U. Schauer, and P. Eriksson, "Atlantic sources of the Arctic Ocean surface and halocline waters," *Polar Research*, vol. 23, no. 2, pp. 181–208, 2004.

[26] N. Untersteiner, "On the mass and heat balance of Arctic sea ice," *Archives for Meteorology, Geophysics and Bioclimatology*, vol. 12, pp. 151–182, 1961.

[27] D. Cavalieri, C. Parkinson, P. Gloersen, and H. J. Zwally, *Updated Yearly. Sea Ice Concentrations from Nimbus-7 SMMR and DMSP SSM/I-SSMIS Passive Microwave Data, 1979–2010*, National Snow and Ice Data Center. Digital Media, Boulder, Colo, USA, 1996.

[28] R. Kwok and G. F. Cunningham, "ICESat over Arctic sea ice: estimation of snow depth and ice thickness," *Journal of Geophysical Research C*, vol. 113, no. 8, Article ID C08010, 2008.

[29] R. Kwok, "Outflow of Arctic ocean sea ice into the Greenland and Barent seas: 1979–2007," *Journal of Climate*, vol. 22, no. 9, pp. 2438–2457, 2009.

[30] S. Smirnov and A. Korablev, "A regional oceanographic database for the Nordic Seas: from observations to climatic dataset," in *Proceedings of the International Conference on Marine Data and Information Systems (IMDIS '10)*, p. 81, Paris, France, March 2010.

[31] I. V. Polyakov, A. Beszczynska, E. C. Carmack et al., "One more step toward a warmer Arctic," *Geophysical Research Letters*, vol. 32, no. 17, Article ID L17605, pp. 1–4, 2005.

[32] I. A. Dmitrenko, I. V. Polyakov, S. A. Kirillov et al., "Toward a warmer Arctic Ocean: spreading of the early 21st century Atlantic water warm anomaly along the Eurasian basin margins," *Journal of Geophysical Research C*, vol. 113, no. 5, Article ID C05023, 2008.

[33] S. Martin and D. J. Cavalieri, "Contribution of the Siberian shelf to the Arctic ocean intermediate and deep water," *Journal of Geophysical Research*, vol. 94, no. 12, pp. 12725–12738, 1989.

[34] V. F. Zakharov, *Sea Ice in the Climate System*, Hydrometeoizdat, St. Petersburg, Russia, 1996.

[35] S. D. Smith, R. D. Muench, and C. H. Pease, "Polynyas and leads: an overview of physical processes and environment," *Journal of Geophysical Research*, vol. 95, no. C6, pp. 9461–9479, 1990.

[36] T. Uttal, J. A. Curry, M. G. McPhee et al., "Surface heat budget of the arctic ocean," *Bulletin of the American Meteorological Society*, vol. 83, no. 2, pp. 255–275, 2002.

[37] I. A. Repina and A. S. Smirnov, "Heat and momentum exchange between the atmosphere and ice from the observational data obtained in the region of Franz Josef Land," *Atmospheric and Ocean Physics*, vol. 36, no. 5, pp. 618–626, 2000.

[38] S. Marcq and J. Weiss, "Influence of sea ice lead-width distribution on turbulent heat transfer between the ocean and the atmosphere," *The Cryosphere*, vol. 6, pp. 143–156, 2012.

[39] K. Aagaard, L. K. Coachman, and E. Carmack, "On the halocline of the Arctic Ocean," *Deep Sea Research A*, vol. 28, no. 6, pp. 529–545, 1981.

[40] I. V. Polyakov, V. A. Alexeev, I. M. Ashik et al., "Fate of early 2000's arctic warm water pulse," *Bulletin of the American Meteorological Society*, vol. 92, no. 5, pp. 561–566, 2011.

[41] I. V. Polyakov, G. V. Alekseev, L. A. Timokhov et al., "Variability of the intermediate Atlantic water of the Arctic ocean over the last 100 years," *Journal of Climate*, vol. 17, no. 23, pp. 4485–4497, 2004.

[42] W. Meier, F. Fetterer, K. Knowles, M. Savoie, and M. J. Brodzik, *Updated Quarterly. Sea Ice Concentrations from Nimbus-7 SMMR and DMSP SSM/I-SSMIS Passive Microwave Data, 2010*, National Snow and Ice Data Center. Digital Media, Boulder, Colo, USA, 2006.

[43] N. V. Koldunov, D. Stammer, and J. Marotzke, "Present-day arctic sea ice variability in the coupled ECHAM5/MPI-OM model," *Journal of Climate*, vol. 23, no. 10, pp. 2520–2543, 2010.

[44] D. P. Dee, S. M. Uppala, A. J. Simmons et al., "The ERA-Interim reanalysis: configuration and performance of the data assimilation system," *Quarterly Journal of the Royal Meteorological Society*, vol. 137, no. 656, pp. 553–597, 2011.